Mendeleev Commun., 2027, **37**, JUST ACCEPTED

Received 18.08.26 26/8179
Revised 08.10.26

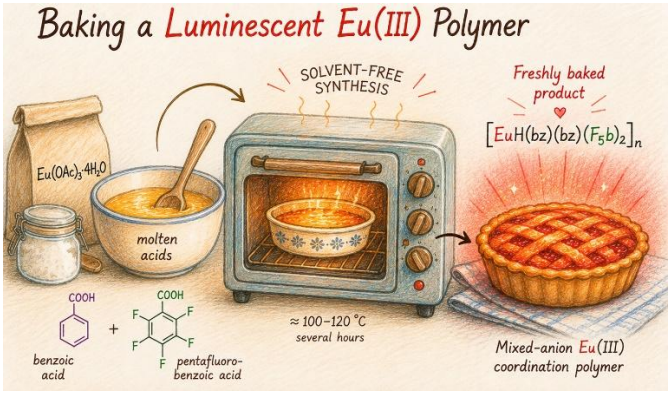
Effective solvent-free synthetic method for obtaining benzoate-pentafluorobenzoate europium(III) compound

Maxim A. Shmelev,[a]* Alena E. Bolot'ko,[a] Evgeniya A. Varaksina,[b] Aleksandr S. Chistyakov,[a] Maria Yu. Boroda,[c] Anastasia A. Levina,[a,d] Andrey V. Lalov,[d] Ilya V. Taydakov,[b] Alexey A. Sidorov[a] and Igor L. Eremenko[a]

[a] *N. S. Kurnakov Institute of General and Inorganic Chemistry, Russian Academy of Sciences, 119071 Moscow, Russian Federation. E-mail: shmelevma@yandex.ru*
[b] *P. N. Lebedev Physical Institute, Russian Academy of Sciences, 119991 Moscow, Russian Federation*
[c] *National Research University Higher School of Economics (HSE University), 101000 Moscow, Russian Federation*
[d] *N. D. Zelinsky Institute of Organic Chemistry, Russian Academy of Sciences, 119991 Moscow, Russian Federation*

DOI: 10.71267/mencom.8179

An effective solvent-free synthetic method for obtaining a mixed-anion europium(III) coordination compound has been proposed. The approach is based on the interaction of europium acetate with molten benzoic H(bz) and pentafluorobenzoic H(F_5b) acids, which allows the preparation of the coordination polymer $[Eu(H(bz))(bz)(F_5b)_2]_n$. The structure, supramolecular arrangement, and photoluminescent properties of the compound significantly differ from those of the previously obtained compounds $[Eu(EtOH)_2(F_5b)(bz)_2]_n$ and $[Eu(EtOH)(F_5b)_2(bz)]_n$ with coordinated ethanol molecules, which were synthesized by conventional methods.



Keywords: mixed-anion compounds, europium(III), solvent-free synthesis, non-covalent interactions, photoluminescence.

Coordination compounds of rare-earth elements (RREs), especially europium(III), have found widespread applications in organic light-emitting diodes (OLEDs), luminescent sensors, and biomarkers[1-4]. Simultaneous incorporation of several carboxylate anions into the coordination environment of lanthanides allows fine tuning of the structures of the resulting compounds, as well as their photoluminescent properties[5-8]. However, the practical application of coordination compounds depends on the availability of reliable synthetic methods that provide reproducible preparation of complexes with a predetermined composition and structure.

The most common approach to the synthesis of RRE coordination compounds is the reaction of various REE salts or hydroxides with organic ligands in water or organic solvents. Despite its versatility, this approach has several limitations. First, the coordination of solvent molecules to REE atoms may lead to significant quenching of the photoluminescence of the resulting compounds via high-frequency oscillators (O-H and C-H), causing nonradiative relaxation of the excited state[9-12]. Moreover, the coordination of solvent molecules to metal ions or their incorporation into the crystal structure as solvate molecules may significantly reduce the stability of the compounds because the removal of solvent molecules frequently leads to amorphization of the product, even at ambient temperature. Attempts to use non-coordinating solvents are often complicated by their low polarity, which may not provide the required solubility of the initial reagents and the resulting compounds. In this context, the development of alternative and effective synthetic methods that eliminate the use of solvents appears to be a relevant scientific objective[13-16].

Previously, we showed that the interaction of europium benzoate (bz) and pentafluorobenzoate (F_5b), depending on the initial reagents ratio, leads to the formation of $[Eu(EtOH)_2(F_5b)(bz)_2]_n$ and $[Eu(EtOH)(F_5b)_2(bz)]_n$. Significant quenching of the photoluminescence of these compounds was observed due to the C-H and O-H vibrations of the coordinated ethanol molecules[17]. In the present work, as an alternative approach to obtaining mixed-anion benzoate-pentafluorobenzoate europium compounds, we investigated the synthesis of these compounds by the interaction of europium acetate with molten benzoic or pentafluorobenzoic acids (solvent-free synthesis), which completely eliminates the coordination of solvent molecules to metal ions.

At the first stage, homoanionic europium benzoates and pentafluorobenzoates were obtained using this approach. Nine equivalents of eihter pentafluorobenzoic acid H(F_5b) or benzoic acid H(bz) were added to europium acetate placed in a glass crystallizing dish, and the reaction mixture was stirred with a glass rod until a homogeneous mass was formed. The resulting reaction mixture was heated to the melting point of the corresponding acid (T_m = 107 °C for H(F_5b)[18] and T_m = 122 °C for H(bz))[19], and dissolution of europium acetate in the melt was observed (Scheme 1). The melt was then heated for 10 hours until the excess subliming acid had been removed, with periodic stirring using a glass rod, resulting in the formation of a homogeneous solid product. According to CHN elemental analysis, the composition of the resulting products agrees well with $\{Eu(F_5b)_3\}$ (**1**) and $\{Eu(bz)_3\}$ (**2**).

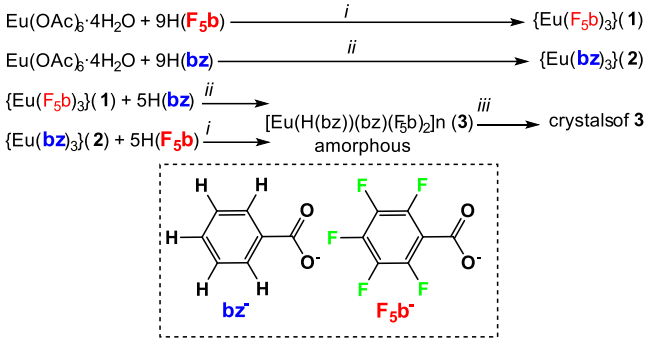
In the second stage, five equivalents of pentafluorobenzoic or benzoic acid were added to the resulting europium benzoate **1** and pentafluorobenzoate **2**, respectively, and the reaction was carried out according to the synthetic procedure described above (Scheme 1). As a result of both reactions, products containing two bz molecules and two F_5b molecules per europium atom, according to CNH elemental analysis, were obtained. This also indicates that one of ligands is present in the protonated form. Since CHN elemental analysis and IR spectroscopy do not allow unambiguous determination of which ligand is protonated, the product composition may correspond to either $\{Eu(H(bz))(F_5b)_2(bz)\}$ or $\{Eu(H(F_5b))(F_5b)(bz)_2\}$. However, the product obtained in the second stage could be recrystallized from dichloromethane, and crystals of $[Eu(H(bz))(bz)(F_5b)_2]_n$ (**3**, Fig. 1) were obtained by slow evaporation of the solvent. This composition is consistent with the CHN elemental analysis data obtained for the product of

© Mendeleev Communications.

the melt synthesis. The phase purity of compound **3** obtained by recrystallization from dichloromethane was confirmed by powder XRD (Fig. S1). According to powder XRD, the product obtained directly by the melt synthesis is X-ray amorphous.

It should be noted that the acidities of benzoic and pentafluorobenzoic acids differ substantially (pKa = 4.2 and 1.6, respectively). Therefore, the formation of the mixed-anion compound 3 upon treatment of a lanthanide benzoate with the stronger pentafluorobenzoic acid is fully expected: the stronger acid readily replaces the weaker one in the coordination sphere of the metal, and the driving force of the substitution is the thermodynamic stability of the resulting mixed-anion product rather than its solubility. In contrast, the reverse reaction - the action of the weaker benzoic acid on a lanthanide pentafluorobenzoate - is far less obvious, since a weaker acid would not normally be expected to protonate the anion of a stronger acid, especially for rare-earth elements, which are among the hardest acids according to Pearson's classification.

IR spectroscopy data (Fig. S2) indicated the replacement of the initial ligands and rearrangement of the europium coordination node. In the range of 1700–1350 cm^{-1}, the bands of the free acetate anion disappear. Instead, a characteristic aryl carboxylate profile is observed, including skeletal vibrations of the conjugated carbon backbone (1450–1700 cm^{-1}) and a high-intensity doublet of the carboxylate anion corresponding to asymmetric (1490–1535 cm^{-1}) and symmetric (1396–1408 cm^{-1}) ν(OCO) vibrations. The presence of bands in the range of 1361–997 cm^{-1} (for complexes **1** and **3**) indicates the presence of C-F bonds directly attached to the ring. The low-frequency region contains bending vibrations of the OCO groups (775–681 cm^{-1}), whose positions are sensitive to the geometry of the Eu-O-C node and indicate a bidentate or bridging coordination mode. Out-of-plane angular deformations of the perfluorinated ring are observed in the range of 960–775 cm^{-1}, which is characteristic of F_5b.



Scheme 1 *i* – 107 °C, *ii* – 122 °C, *iii* – CH_2Cl_2.

In the structure of coordination polymer **3**, binuclear {Eu_2} fragments can be distinguished, in which the metal atoms are linked to each other by two bridging and two chelate-bridging F_5b anions (Eu-O 2.345(5)-2.631(4) Å). The binuclear fragments are, in turn, linked to each other by two μ_2-η^2-benzoate anions (Eu-O 2.397(4) Å, 2.408(4) Å), forming a distorted chain-like polymer (Fig. 1; Eu···Eu distances are 3.919 (1) Å, 4.007 (1) Å, and the Eu···Eu···Eu angle is 160.36(3)°). Each europium atom completes its coordination environment to a triangular dodecahedron (EuO_8) through the coordination of a monodentate benzoic acid molecule (Eu-O 2.325(5) Å). The polymer chains of compound **3** are additionally stabilized by numerous π···π interactions between F_5b and bz anions or coordinated H(bz) molecules (Fig. S3, Table S1), as well as by multiple C-F···π interactions between fluorine atoms of the F_5b anions and the aromatic systems of the bz anions or coordinated H(bz) molecules (Fig. S3, Table S2). The polymer chains are further connected into supramolecular layers through C-H···O and C-H···F interactions (Table S3).

In comparison with the previously obtained compounds $[Eu(EtOH)_2(F_5b)(bz)_2]_n$ and $[Eu(EtOH)(F_5b)_2(bz)]_n$[17], the geometry of the polymer chain in compound **3** differs significantly. Thus, a change in the coordination modes of benzoate and pentafluorobenzoate anions to the europium atom is observed, which leads to a decrease in the Eu···Eu distances by approximately 1 Å on average. The replacement of ethanol molecules by a coordinated benzoic acid molecule results in a significant rearrangement of the non-covalent interaction system and the formation of multiple π···π interactions, which were absent in the previously synthesized compounds.

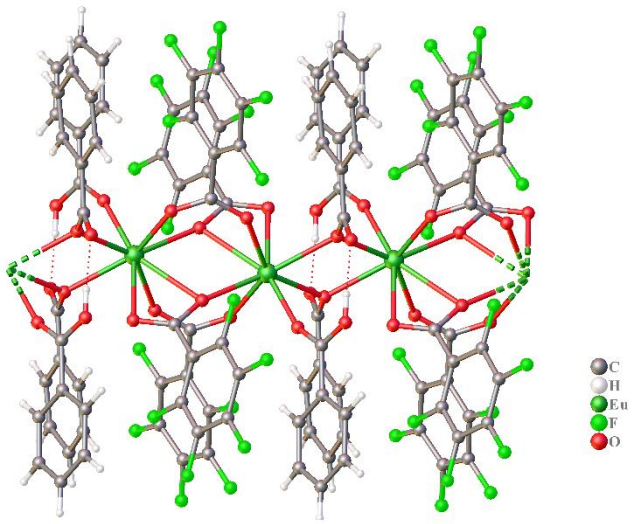


Figure 1. Fragment of the polymer chain in compound **3**. Hydrogen bonds are shown as dashed lines.

At the next stage, an attempt was made to obtain a mixed-anion benzoate-pentafluorobenzoate compound with 1,10-phenanthroline molecules. The addition of three equivalents of 1,10-phenanthroline to $[Eu(H(bz))(bz)(F_5b)_2]_n$ (**3**), followed by heating of the reaction mixture to the melting point of phenanthroline (117 °C), led to the immediate formation of a dark-brown vitreous solid. Variation of the reagent ratio also resulted in glass formation.

The luminescence spectra of europium complexes **1-3** were recorded at 77 and 300 K (Figs. 2 and S4). For compound **3**, the photoluminescent properties were investigated for a sample obtained by recrystallization from methylene chloride. Complex **2** exhibits the most pronounced splitting, with at least 6 resolved components for the both $^5D_0 \rightarrow {}^7F_1$ and $^5D_0 \rightarrow {}^7F_2$ transitions, exceeding the maximum number of Stark components $2J+1$, expected for a single Eu^{3+} coordination site. This observation suggests the presence of multiple spectroscopically non-equivalent Eu^{3+} centers contributing to the emission spectrum. In contrast, the number of resolved Stark components for complexes **1** and **3** does not exceed the theoretical limit, indicating a more homogeneous local environment of the Eu^{3+} ions.

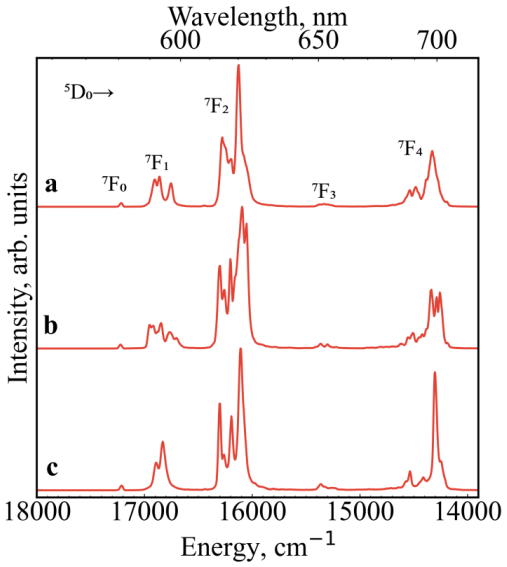


Figure 2. Photoluminescence spectra of **1** (a), **2** (b) and **3** (c) recorded at 77 K upon excitation at 280 nm.

The splitting pattern of the Eu^{3+} emission transitions is consistent with the local symmetry of the coordination environment. For complex **3**, the $^5D_0 \rightarrow {}^7F_0$ transition appears as a single line, the $^5D_0 \rightarrow {}^7F_1$ transition is split

© Mendeleev Communications.

into two components, whereas the $^5D_0 \rightarrow {}^7F_2$ transition exhibits four components. This pattern is characteristic of a D_{2d} local symmetry of the Eu^{3+} ion[20], obtained by the single-crystal X-ray diffraction data. The intensity ratio of the electric dipole $^5D_0 \rightarrow {}^7F_2$ transition to the magnetic dipole $^5D_0 \rightarrow {}^7F_1$ decreases from 5.47 and 4.73 in the previously investigated complexes $[Eu(EtOH)_2(F_5b)(bz)_2]_n$ and $[Eu(EtOH)(F_5b)_2(bz)]_n$[17], respectively, to 3.78 in the ethanol-free analogue $Eu(H(bz))(bz)(F_5b)_2]_n$, indicating a more centrosymmetric Eu^{3+} environment in the latter.

The excitation spectra of complexes **1-3** recorded upon monitoring the $^5D_0 \rightarrow {}^7F_2$ emission are shown in Figs. 3, S5 and S6. All three compounds exhibit broad ligand-centred excitation bands extending up to approximately 28000 cm^{-1}, consistent with the coordination of the benzoate and pentafluorobenzoate ligands to the Eu^{3+} ions. This observation is in agreement with the IR spectroscopic data and confirms the formation of the corresponding europium carboxylate complexes. In addition, the excitation spectra display intense intraconfigurational 4f-4f absorption bands of Eu^{3+}, corresponding to direct excitation of the metal ion.

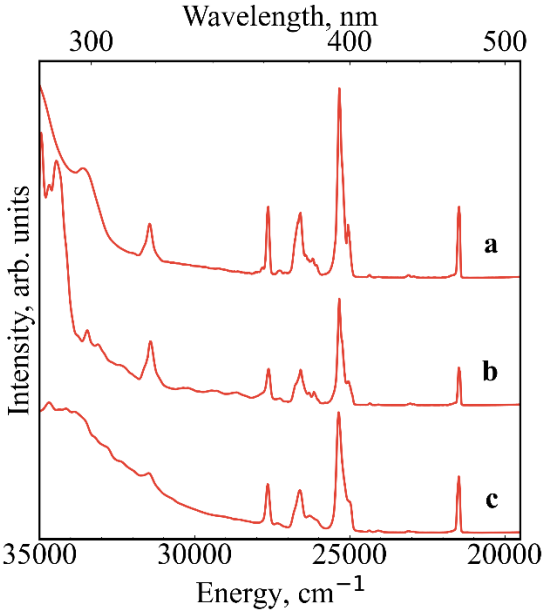


Figure 3. Photoluminescence excitation spectra of 1 (a), 2 (b) and 3 (c) recorded at 77 K with emission monitored at 615 nm.

Complexes **1-3** exhibit similar intrinsic luminescence quantum yields (Table 1), indicating comparable relaxation processes of Eu^{3+} ion. Thus, the ligand environment has a similar effect on the radiative and non-radiative deactivation of the emitting $^5D_0$ state in all three compounds. In contrast, the previously reported mixed-anion complexes $[Eu(EtOH)_2(F_5b)(bz)_2]_n$ and $[Eu(EtOH)(F_5b)_2(bz)]_n$ exhibited substantially faster non-radiative deactivation of the Eu^{3+} excited state, which was attributed to quenching by coordinated ethanol molecules. This assumption is supported by comparison with the solvent-free mixed-anion polymer $[Eu(H(bz))(bz)(F_5b)_2]_n$ (**3**), in which the non-radiative decay rate of the $^5D_0$ state is more than two times lower than in the ethanol-containing analogues.

Notably, complex **2** exhibits the highest overall luminescence quantum yield among the studied compounds. This enhancement arises from both the highest intrinsic Eu^{3+} luminescence quantum yield and the most efficient ligand-to-metal energy transfer. In contrast, the pentafluorobenzoate complex **1** demonstrates markedly lower sensitization efficiency. This decrease is likely associated with the higher energy of the ligand triplet state of F_5b compared with that of bz (22300 and 21300 cm^{-1}, respectively[21, 22]). This may reduce the overlap between the ligand and metal excited-state manifolds, leading to less efficient ligand-to-lanthanide energy transfer.

Table 1. Radiative (A_{rad}) and non-radiative (A_{nrad}) rate constants, observed lifetimes (τ^{obs}), sensitisation efficiencies (η_{sens}), and absolute (Q_{Ln}^{Ln}) and intrinsic (Q_L^{Ln}) quantum yields for complexes **1-3**, $[Eu(EtOH)_2(F_5b)(bz)_2]_n$, and $[Eu(EtOH)(F5b)_2(bz)]_n$ [17].

Compound	A_{rad}, s^{-1}	A_{nrad}, s^{-1}	τ^{obs}, ms		Q_{Ln}^{Ln}, %	Q_L^{Ln}, %	η_{sens}, %
			T=300K	T=77K			
$\{Eu(F_5b)_3\}$ (**1**)	386	444	1205	1195	46	5	11
$\{Eu(bz)_3\}$ (**2**)	417	367	1275	1330	53	33	62
$[Eu(H(bz))(bz)(F_5b)_2]_n$ (**3**)	364	432	1255	1245	46	23	50
$[Eu(EtOH)_2(F_5b)(bz)_2]_n$	380	1010	715	700	27		
$[Eu(EtOH)(F_5b)_2(bz)]_n$	380	800	850	1485	32		

Thus, an effective solvent-free synthetic method for obtaining europium coordination compounds based on the interaction of europium acetate with organic acids in their molten state has been developed. This approach allows avoiding the issues associated with the coordination of solvent molecules to rare-earth atoms and luminescence quenching, which are typical for compounds obtained by conventional synthesis in organic solvents. Compared with the previously synthesized benzoate-pentafluorobenzoate compounds containing coordinated ethanol molecules $[Eu(EtOH)_2(F_5b)(bz)_2]_n$ and $[Eu(EtOH)(F_5b)_2(bz)]_n$, compound $[Eu(H(bz))(bz)(F_5b)_2]_n$ (**3**) demonstrates a rearrangement of the polymer chain geometry, changes in the contribution of different non-covalent interactions to the stabilization of polymer chains and supramolecular structure, as well as a significant enhancement of the main photoluminescence characteristics. These results demonstrate the potential of the proposed synthetic approach for obtaining compounds with improved functional properties.

The study was supported by the Russian Science Foundation grant No. 25-73-10110, https://rscf.ru/en/project/25-73-10110/.

IR spectroscopy, X-ray diffraction, powder X-ray diffraction and CHN analyses of the complexes were performed using the equipment of the JRC PMR IGIC RAS as part of the state assignment of the IGIC RAS in the field of fundamental scientific research. Photophysical measurements were carried out with financial support from the Ministry of Science and Higher Education of the Russian Federation, using the equipment of the Research Center for Molecular Structure Studies, INEOS RAS.

Crystallography in the Manuscript. Details of the data collection see below.†

Online Supplementary Materials

Supplementary data associated with this article can be found in the online version at doi: 10.71267/mencom.8179

†Single crystal X-ray diffraction analysis of compound 3 was performed on a Bruker D8 Venture diffractometer equipped with a CCD detector (MoKα, λ = 0.71073 Å; graphite monochromator). A semi-empirical absorption correction using the SADABS[23] program was applied to all compounds. Using Olex2[24], the structure was solved with a ShelXS structure solution program using Direct Methods and refined using a ShelXL[25] refinement package with the Least Squares minimization in anisotropic approximation for nonhydrogen atoms. The hydrogen atom of the OH group was located from a difference Fourier synthesis, whereas the remaining hydrogen atoms were placed in calculated positions and refined using the riding-model approximation with isotropic displacement parameters. The geometry of metal polyhedra was determined using the program SHAPE 2.1[26].

CCDC 2574270 (3) contain the supplementary crystallographic data for this paper. These data can be obtained free of charge from The Cambridge Crystallographic Data Centre via http://www.ccdc.cam.ac.uk.

Crystal data for **3**. $C_{28}H_{11}EuF_{10}O_8$ (M = 817.33), T = 100 K, monoclinic space group $P2_1/c$, a = 7.8103(14), b = 14.715(3), c = 23.030(5) Å, β = 93.327(5) °, V = 2642.4(9) Å^3, Z = 4, μ(MoKa) = 2.498 mm^{-1}. At the angles 2.248 < θ < 26.012 °, total of 15368 reflections were measured, including 5170 unique reflections (R_{int} = 0.0794) and 3850 reflections with $I > 2\sigma(I)$, which were used in all calculations. The final R_1 = 0.0761, wR_2 = 0.0999 (all data) and R_1 = 0.0516, wR_2 = 0.0909 [$I > 2\sigma(I)$], $GOOF$ = 1.037. Largest diff. peak/hole -1.352 and 1.209 eÅ^{-3}.

© Mendeleev Communications.

References

1. P. Su, F. Song, J. Cao, C. H. Yan, Y. Tang, *Acc. Chem. Res.*, 2025, **58(2)**, 218-230. https://doi.org/10.1021/acs.accounts.4c00649;
2. N. Song, C. Wang, Y. Tang, *CS Appl. Mater. Interfaces.*, 2025, **17(48)**, 65386-65398. https://doi.org/10.1021/acsami.5c20695;
3. M. A. Shmelev, R. A. Polunin, N. V. Gogoleva, I. S. Evstifeev, P. N. Vasilyev, A. A. Dmitriev, E. A. Varaksina, N. N. Efimov, I. V. Taydakov, A. A. Sidorov, M. A. Kiskin, N. P. Gritsan, S. V. Kolotilov, I. L. Eremenko, *Molecules*, 2021, **26(14)**, 4296. https://doi.org/10.3390/molecules26144296;
4. Y. A. Bryleva, A. V. Mikheylis, A. M. Agafontsev, L. A. Glinskaya, A. V. Tkachev, J. Lumin., 2025, **281**, 121144. https://doi.org/10.1016/j.jlumin.2025.121144
5. A. E. Bolot'ko, M. A. Shmelev, A. S. Chistyakov, J. K. Voronina, E. A. Varaksina, N. V. Gogoleva, I. L. Eremenko, *Dalton Trans.*, 2025, **54(14)**, 5708-5720. https://doi.org/10.1039/d4dt03414g;
6. M. A. Shmelev, G. N. Kuznetsova, N. V. Gogoleva, F. M. Dolgushin, Y. V. Nelyubina, M. A. Kiskin, A. A. Sidorov, I. L. Eremenko, *Russ.Chem.Bull*, 2021, **70(5)**, 830-838. https://doi.org/10.1007/s11172-021-3156-9;
7. M. A. Shmelev, N. V. Gogoleva, A. A. Sidorov, M. A. Kiskin, J. K. Voronina, Y. V. Nelyubina, E. A. Varaksina, V. M. Korshunov, I. V. Taydakov, I. L. Eremenko, *Inorg. Chim. Acta.*, 2021, **515**, 120050. https://doi.org/10.1016/j.ica.2020.120050
8. E. A. Sanzhenakova, K. S. Smirnova, I. P. Pozdnyakov, A. S. Berezin, V. I. Potkin, E. V. Lider, *Dalton Trans.*, 2025, **54(19)**, 7810-7818. https://doi.org/10.1039/d5dt00127g
9. R. R. Fonseca, R. D. Gaspar, I. M. Raimundo Jr, P. P. Luz, *J. Rare Earths*, 2019, **37(3)**, 225-231. https://doi.org/10.1016/j.jre.2018.07.006;
10. Z. Ahmed, K. Mahiya, K. Iftikhar, *Inorg. Chim. Acta.*, 2022, **541**, 121086. https://doi.org/10.1016/j.ica.2022.121086;
11. R. Shi, A. V. Mudring, *ACS Mater. Lett.*, 2022, **4(10)**, 1882-1903. https://doi.org/10.1021/acsmaterialslett.2c00595;
12. M. A. Shmelev, N. V. Gogoleva, F. M. Dolgushin, K. A. Lyssenko, M. A. Kiskin, E. A. Varaksina, I. V. Taidakov, A. A. Sidorov, I. L. Eremenko, *Russ J Coord Chem.*, 2020, **46(7)**, 493-504. https://doi.org/10.1134/S1070328420070076
13. J. Cepeda, S. Pérez-Yáñez, G. Beobide, O. Castillo, J. Á. García, M. Lanchas, A. Luque, *Dalton Trans.*, 2015, **44(15)**, 6972-6986. https://doi.org/10.1039/c4dt03797a;
14. J. Liu, L. Pei, Z. Xia, Y. Xu, *Cryst. Growth Des.*, 2019, **19(11)**, 6586-6591. https://doi.org/10.1021/acs.cgd.9b01014
15. N. K. Singh, S. Gupta, V. K. Pecharsky, V. P. Balema, *J. Alloys Compd.*, 2017, **696**, 118-122. https://doi.org/10.1016/j.jallcom.2016.11.220
16. A. S. Zaguzin, P. A. Abramov, M. I. Rakhmanova, A. N. Usoltsev, M. N. Sokolov, V. P. Fedin, S. A. Adonin, *Polyhedron*, 2024, **253**, 116908. https://doi.org/10.1016/j.poly.2024.116908
17. M. A. Shmelev, A. A. Levina, A. S. Chistyakov, E. A. Varaksina, J. K. Voronina, G. A. Razgonyaeva, I. V. Taidakov, A. A. Sidorov, I. L. Eremenko, *Mendeleev Commun.*, 2025, **35(1)**, 35-38. https://doi.org/10.71267/mencom.7566
18. G. K. S. Prakash, J. Hu. Pentafluorobenzoic acid. In: Encyclopedia of Reagents for Organic Synthesis. Chichester, UK: John Wiley & Sons, Ltd, 2006. https://doi.org/10.1002/047084289X.rn00682.
19. G. Indrayanto, A. Syahrani, A. Rahman, W. Tanudjojo, S. Susanti, M. Yuwono, S. Ebel, Benzoic acid. In *Analytical profiles of drug substances and excipients,* Elsevier, Edited by Harry G. Brittain, 1999, **26**, 1-46. https://doi.org/10.1016/S0099-5428(08)60620-6
20. K. Binnemans, *Coord. Chem. Rev.*, 2015, **295**, 1-45. https://doi.org/10.1016/j.ccr.2015.02.015
21. E. A. Mikhalyova, A. V. Yakovenko, M. Zeller, K. S. Gavrilenko, M. A. Kiskin, S. S. Smola, V. P. Dotsenko, I. L. Eremenko, A. W. Addison, V. V. Pavlishchuk, *Dalton Trans*, 2017, **46(11)**, 3457-3469. https://doi.org/10.1039/c6dt04757b
22. W. X. Li, W. J. Chai, X. J. Sun, T. Ren, X. Y. Shi, *J. Fluoresc.*, 2010, **20(4)**, 873-880. https://doi.org/10.1007/s10895-010-0633-1
23. R.H. Blessing, *Acta Cryst A.* 1995, **A51**, 33. https://doi.org/10.1107/S0108767394005726
24. O. V. Dolomanov, L. J. Bourhis, R. J. Gildea, J. A. K. Howard, H. Puschmann, *J. Appl. Crystallogr.*, 2009, **42**, 339–341. https://doi.org/10.1107/S0021889808042726
25. G. M. Sheldrick, *Acta Crystallogr. C*, 2015, **71**, 3–8. https://doi.org/10.1107/S2053229614026540
26. D. Casanova, M. Llunell, P. Alemany, S. Alvarez, *Chem. Eur. J.,* 2005, **11**, 1479. https://doi.org/10.1002/chem.200400799

Received: 18th August 2026; Com. 26/8179

© Mendeleev Communications.